MOLECULAR AND CELLULAR BIOLOGY, June 2007, p. 4454–4464 Vol. 27, No. 12
0270-7306/07/$08.00+0 doi:10.1128/MCB.00133-07

Viable Mice with Compound Mutations in the Wnt/Dvl Pathway Antagonists *nkd1* and *nkd2*▽

Shu Zhang,[1] Tolga Çagatay,[1] Manami Amanai,[1]§ Mei Zhang,[1]¶ Janine Kline,[4]‡ Diego H. Castrillon,[1] Raheela Ashfaq,[1] Orhan K. Öz,[3] and Keith A. Wharton, Jr.[1,2]*

Department of Pathology,[1] Department of Molecular Biology,[2] and Department of Radiology,[3] University of Texas Southwestern Medical Center, Dallas, Texas 75390, and Department of Developmental Biology, Howard Hughes Medical Institute, Beckman Center, Stanford University School of Medicine, Stanford, California 94305[4]

Received 21 January 2007/Returned for modification 27 February 2007/Accepted 22 March 2007

Gradients of Wnt/β-catenin signaling coordinate development and physiological homeostasis in metazoan animals. Proper embryonic development of the fruit fly *Drosophila melanogaster* requires the Naked cuticle (Nkd) protein to attenuate a gradient of Wnt/β-catenin signaling across each segmental anlage. Nkd inhibits Wnt signaling by binding the intracellular protein Dishevelled (Dsh). Mice and humans have two *nkd* homologs, *nkd1* and *nkd2*, whose encoded proteins can bind Dsh homologs (the Dvl proteins) and inhibit Wnt signaling. To determine whether *nkd* genes are necessary for murine development, we replaced *nkd* exons that encode Dvl-binding sequences with *IRES-lacZ/neomycin* cassettes. Mutants homozygous for each nkd^{lacZ} allele are viable with slightly reduced mean litter sizes. Surprisingly, double-knockout mice are viable, with subtle alterations in cranial bone morphology that are reminiscent of mutation in another Wnt/β-catenin antagonist, *axin2*. Our data show that *nkd* function in the mouse is dispensable for embryonic development.

Our expanding knowledge of molecular mechanisms that govern vertebrate development stems from a legacy of discovery using model genetic organisms—in particular, the fruit fly *Drosophila melanogaster*. Just over a quarter century ago, Nüsslein-Volhard, Wieschaus, and their colleagues in Tübingen saturated the fly genome with embryonic lethal mutations that produce altered body patterns, the cloning of which ultimately revealed an evolutionarily conserved "toolkit" of genes—composed predominantly of transcription factors and signal transducers—that executes the development of all of the animals studied to date (8, 55). Because teleost fish—from which modern mammals derive—underwent two rounds of genome duplication 300 to 400 million years ago (27), genes that are present in single copy in protostomes such as *Drosophila* are often present in multiple copies and act with partial or complete redundancy in mammals. For example, mammals have three *hedgehog* (*hh*) and four *Notch* (*N*) genes, each of which is present in single copy in flies (2, 29, 48). Duplicate toolkit genes may evolve mutable tissue- or stage-specific functions or may exhibit functional redundancy that is not evident unless all paralogs are simultaneously mutated.

Wnt proteins are a family of intercellular signaling proteins with widespread roles in animal development, tissue homeostasis, and human disease (11, 47). Flies have 7 *wnt* genes, while mice and humans have 19 (http://www.stanford.edu/~rnusse/wntwindow.html). Diversification of Wnt proteins occurred early in animal evolution, as the basal cnidarian *Nematostella vectensis* has 12 *wnt* genes whose expression in discrete domains along the anterior-posterior axis is reminiscent of fly and mammalian homeotic gene expression (41). Fundamental insights into the mechanism of Wnt signaling emerged from the study of *wingless* (*wg*), a *Drosophila wnt* gene with numerous sequential roles in nearly all of the tissues and life stages of the fly (37). The earliest requirement for *wg* is during embryo segmentation, where its expression in ectodermal stripes prefigures the segmented body plan (3, 52). When the secreted Wg protein encounters adjacent cells, it elicits a complex signaling cascade, termed the canonical Wnt/β-catenin pathway, that culminates in accumulation of the transcriptional cofactor β-catenin and transactivation of tissue-specific target genes (54, 56, 61). Proper embryonic development requires the graded action of Wg and other signals across each segmental anlage (4, 24, 58). In the absence of *wg* or key downstream signal transducers, the transcription of target genes such as *hh* and *engrailed* (*en*) ceases, with dramatic consequences for pattern formation; conversely, increased Wg signaling leads to expanded domains of *hh* and *en* expression, with opposite but equally dramatic phenotypic consequences (4, 5, 43, 52, 53, 60, 62, 75). Subsequent investigations of Wg and other Wnt proteins have revealed several "noncanonical" signaling pathways, some of which, like the canonical pathway, act through Frizzled (Fz) and Arrow/LRP receptors, some of which may act through Fz and cadherin-family molecules, and others of which act through N or Ryk/Derailed (Drl) receptors (12, 16, 25, 30, 39, 40, 49, 63, 65).

Among the original Tübingen mutant collection is the *naked cuticle* (*nkd*) gene (34). Shortly after the onset of Wg action,

* Corresponding author. Mailing address: Laboratory of Molecular Pathology, Department of Pathology, 5323 Harry Hines Blvd. NB6.440, Dallas, TX 75390-9072. Phone: (214) 648-1959. Fax: (214) 648-4070. E-mail: Keith.Wharton@UTSouthwestern.edu.

§ Present address: Laboratory of Mammalian Molecular Embryology, RIKEN Center for Developmental Biology, Kobe 650-0047, Japan.

¶ Present address: Division of Cardiology, Department of Medicine, Duke University Medical Center, Durham, NC 27710.

‡ Present address: Novartis, Emeryville, CA 94601.

▽ Published ahead of print on 16 April 2007.

nkd mutants develop markedly elevated levels of β-catenin and expanded domains of Wg target gene expression despite an apparently normal quantity and distribution of Wg, suggesting that *nkd* mutant cells are hypersensitive to Wg (5, 52, 67, 75). Molecular characterization of *nkd* revealed a novel gene whose transcript is Wg inducible, thereby forming a negative feedback loop (75). Nkd can bind and inactivate Dishevelled (Dsh) or its mammalian homologs, the Dvl proteins, a family of intracellular "scaffold" proteins that transduces several types of Wnt signal but whose mechanisms of action remain mysterious and controversial (7, 51, 57, 68–71). Although Dsh is thought to be a hub of cytoplasmic signaling, a recent report suggests that Dsh may also carry Wnt signals into the nucleus (32). Likewise, the mechanism of Nkd action on Dsh in *Drosophila* remains puzzling but also involves nuclear transport (67).

Mice and humans have two *nkd* genes, *nkd1* and *nkd2*, that share sequence similarity with fly *nkd* in two regions: an EF hand-containing domain—termed the EFX domain—that binds Dsh and a C-terminal histidine-rich region (35, 70–72). Alignments of insect and mammalian Nkd proteins reveal four conserved sequence motifs interspersed by mostly unrelated sequence, suggesting a common arrangement of functional motifs in the ancestral Nkd protein (67, 70). Our studies of *Drosophila* Nkd showed that protein truncations N terminal of Dsh-binding regions produced embryonic lethality with the strongest phenotypic consequences (67, 75). Similarly, mutation or deletion of the mouse Nkd1 EF hand impaired the mutant protein's ability to inhibit Wnt/β-catenin signaling in cultured cells (71). We hypothesized that truncating mutations similar to those that cause strong *nkd* phenotypes and lethality in *Drosophila*, when introduced into the mammalian *nkd* genes, would produce null genetic lesions, possibly resulting in embryonic lethality and/or phenotypes indicative of increased Wnt signaling.

Here we report the generation of mice in which an internal ribosome entry site–β-galactosidase (*IRES-lacZ*) fusion gene replaces exons encoding *nkd1* or *nkd2* EFX domains and the results of our breeding experiments. Each nkd^{lacZ} mouse expresses β-galactosidase in patterns that mimic endogenous *nkd* expression (70). Mice homozygous for each of our nkd^{lacZ} alleles are viable, with slight reductions in mean litter size. Our *nkd1* mutant mice do not exhibit the reduced testis mass that was observed in mice homozygous for a distinct *nkd1* allele reported by another group during the course of our studies (45). By mating *nkd1* to *nkd2* mutant mice in a mixed genetic background, we have obtained a small number of adult homozygous double-mutant mice that are viable and fertile. Unlike the strict genetic requirement for *nkd* in the fly embryo, mouse *nkd* activity is apparently dispensable for embryonic development.

MATERIALS AND METHODS

Animals. All of the experiments in this study were performed according to guidelines approved by the Institutional Animal Care and Use Committee (IACUC).

Cloning of *nkd1* and *nkd2* genomic DNAs. Bacterial artificial chromosome clones encompassing the mouse *nkd1* and *nkd2* coding regions were obtained from mouse 129Sv libraries by Southern blotting and PCR screens performed by Research Genetics (now owned by Invitrogen). Each bacterial artificial chromosome was digested with restriction enzymes, and DNA fragments hybridizing to *nkd1* or *nkd2* cDNA probes by Southern blotting were subcloned into Bluescript-IIKS+ (Stratagene). Subclones encompassing exons 5 to 10 (*nkd1*) or 4 to 10 (*nkd2*) were restriction mapped with multiple six-cutter enzymes, and genomic maps consistent with the Celera mouse genomic sequence were assembled as shown in Fig. 1A and 2A.

Targeting constructs. We used the targeting vector pGKneoTK3.IRESlacZ made by Andreas Kispert (cited in reference 76). For the 5′ arm of *nkd1*, a 1.2-kb SalI/XhoI PCR product that introduced a stop codon at amino acid 91 in exon 5 was cloned into the SalI site; for the 3′ arm, a 3-kb SspI/HindIII fragment within the 3′ untranslated region was cloned into the NotI/BamHI site to make the construct shown in Fig. 1A. For the 5′ arm of *nkd2*, a 0.8-kb SalI/XhoI PCR product that introduced a stop codon into exon 6 at amino acid 121 was cloned into the SalI site; for the 3′ arm, a 2.2-kb SacI/NcoI fragment encompassing exons 8 to 10 was cloned into the NotI/BamHI site to make the construct shown in Fig. 2A.

ES cell culture. SalI-linearized targeting constructs for each gene were electroporated into 129SvEv embryonic stem (ES) cells by standard methods, the cells were subjected to positive and negative selection, and surviving clones were screened by PCR. The targeting frequencies were as follows: *nkd1*, 2/900 clones; *nkd2*, 4/1,460 clones. Each was verified by PCR and Southern blotting with 5′ and 3′ probes external to each targeting arm as shown in Fig. 1A and 2A.

Chimeric-mouse generation. Chimeric mice were generated from two independent ES cell clones for each gene (*nkd1*, 1G3 and 3H7; *nkd2*, 5C12 and 9H3), and similar genotyping, expression, and breeding results were obtained for each clone. The $nkd1^{lacZ}$ and $nkd2^{lacZ}$ mice generated in this study have been deposited and are available through Jackson Laboratories (stock no. 6958 and 6960).

Southern blotting. Tail DNA was digested with EcoRV or EcoRI (for *nkd1*) or XbaI (for *nkd2*) at 37°C overnight, separated on a 0.8% agarose gel, transferred to Hybond-N+ (Amersham Pharmacia Biotech) membrane by alkaline transfer, probed with the indicated ^{32}P-labeled DNA fragments schematized in Fig. 1A and 2A, and exposed for autoradiography.

PCR genotyping. The wild-type *nkd1* allele was detected with primers from intron 4 (N1-IN4-5p, CCTGCTGAAGTGGTTGGTAG) and exon 5 (N1-EX5-3p, GAGAACTCCTCCCATTTAGATG) to generate a 487-bp product, while the recombined $nkd1^{lacZ}$ allele was detected with primer N1-IN4-5p and a primer from the *IRES-lacZ* vector (ILZ-3p, TAGAGCGGCCTACGTTTAAACATCG) to generate a 346-bp product. The wild-type *nkd2* allele was detected with primers in intron 5 (N2-IN5-5p, TGGTCAGGGAACGACAGAG) and exon 6 (N2-IN6-3p, GTTCCAGATCTCAAGAGGTC) to generate a 472-bp product, while the recombined $nkd2^{lacZ}$ allele was detected with primers N2-IN5-5p and ILZ-3p to generate a 346-bp product. PCR amplification of genomic DNA was performed with 35 cycles of denaturation at 94°C, annealing at 58°C, and extension at 72°C, and DNA was visualized on a 1.2% agarose gel with ethidium bromide as shown in Fig. 1C and 2C.

Northern blotting. Mouse tissues were flash frozen in liquid N_2 and Dounce homogenized, and RNA was isolated by the protocol provided with the TRIzol reagent (Invitrogen). Oligo(dT)-selected mRNA was separated on a 1% agarose gel in morpholinepropanesulfonic acid (MOPS) buffer, transferred to Hybond-N+ membrane, and hybridized to ^{32}P-labeled DNA probes as shown in Fig. 1D.

Reverse transcription (RT)-PCR. RNA was isolated from mouse brain of the genotypes indicated in Fig. 2D as described above, reverse transcribed with Moloney murine leukemia virus reverse transcriptase (Invitrogen), and subject to PCR as follows. *nkd2* exons 4 to 7 were detected with exon 4 (N2-EX4-5p, AGGAGCTGCTCAATGGAGA) and exon 7 (N2-EX7-3p, ACCTCGTAGAT GGTGTGCAT) primers to synthesize a 323-bp product; exons 8 to 10 were detected with exon 8 (N2-EX8-5p, CGTGGCAGAACAGAGATTG) and exon 10 (N2-EX10-3p, TACCGCTTGTGACCATAGG) primers to synthesize a 579-bp product; and exons 4 to 10 were detected with primers N2-EX4-5p and N2-EX10-3p to synthesize a 1,025-bp product from the wild-type chromosome or a 699-bp product from the $nkd2^{lacZ}$ chromosome. Sequencing of the 699-bp band from $nkd2^{lacZ/lacZ}$ animals confirmed splicing between exons 5 and 9 that predicts the synthesis of an out-of-frame, prematurely truncated protein (data not shown).

Western blotting. Embryos of each genotype at 15.5 days postcoitus (dpc) were pulverized in liquid N_2 and then homogenized with a Teflon-glass homogenizer in triple-detergent buffer (50 mM Tris, 50 mM NaCl [pH 7.4], 1% NP-40, 0.1% sodium dodecyl sulfate, 0.5% Na-deoxycholate, 5 mM EDTA, 1 mM EGTA, 1 mM Na-orthovanadate, 50 mM NaF, 1× complete protease inhibitor [Roche]), and extracts were spun at 1,000 × *g* for 10 min. A 200-μg sample of soluble extract, quantitated by Bradford assay (Bio-Rad), was resolved by sodium dodecyl sulfate–10% polyacrylamide gel electrophoresis and transferred to polyvinylidene difluoride membranes (Millipore). Membranes were blocked in 5% dry milk for 1 h at room temperature and then incubated with a rabbit polyclonal antibody against Nkd1 (1:1,000; Cell Signaling Technology) or four different Nkd2 antibodies (one made by the University of Texas [UT] Southwestern

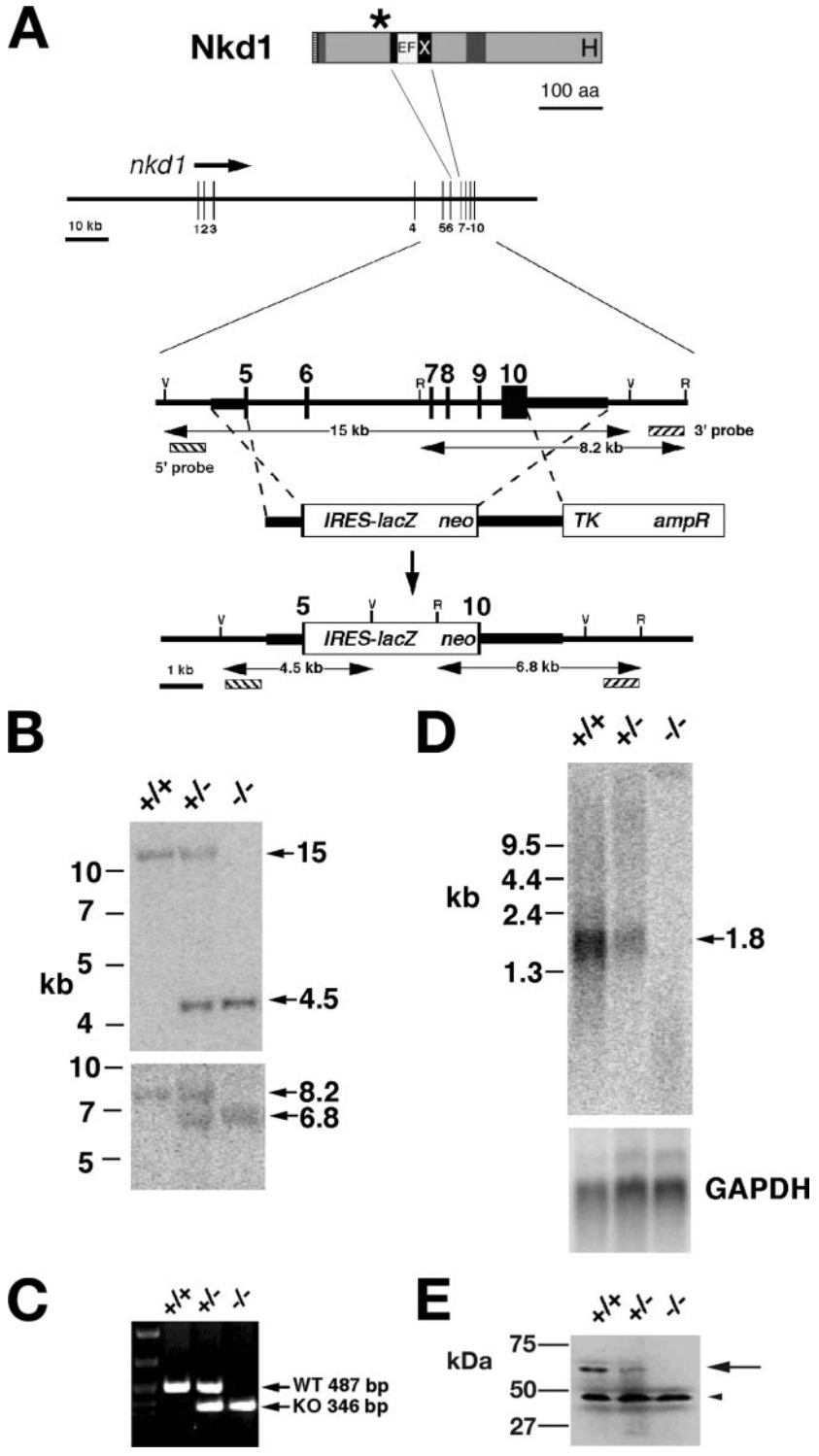

FIG. 1. Targeting of mouse *nkd1*. (A) Schematic of the Nkd1 protein above the genomic region, with exons numbered 1 to 10 and the direction of transcription designated by the arrow. The asterisk designates the position of the stop codon introduced into exon 5. Homologous recombination (dashed lines) replaced exons 5 to 10 with the *IRES-lacZ/neo* cassette. Enzyme sites: V, EcoRV; R, EcoRI. aa, amino acids. (B) Southern blotting of mouse tail DNA cut with EcoRV (top) or EcoRI (bottom) from the indicated genotypes and probed with the 5′ (top) or 3′ (bottom) external probes as designated in panel A. (C) PCR genotyping with tail DNAs from mice of the indicated genotypes amplified with primers specific for the wild-type (WT) and *nkd1*^{lacZ} (KO) chromosomes. (D) Northern blotting of adult lung mRNAs from mice of the indicated genotypes probed with *nkd1* exon 10 probe (top) and then stripped and reprobed with *gapdh* as a loading control (bottom). Note that +/− has approximately half the signal from the major 1.8-kb band of +/+ mice and that −/− lung tissue has no specific hybridization signal. (E) Western blotting of extracts from 15.5-dpc *nkd1* +/+, +/−, and −/− mouse embryos. Note the reduction of the ~60-kDa band in the +/− lane and its absence from the −/− lane (arrow). The arrowhead designates a cross-reactive band that confirms equal loading in each lane.

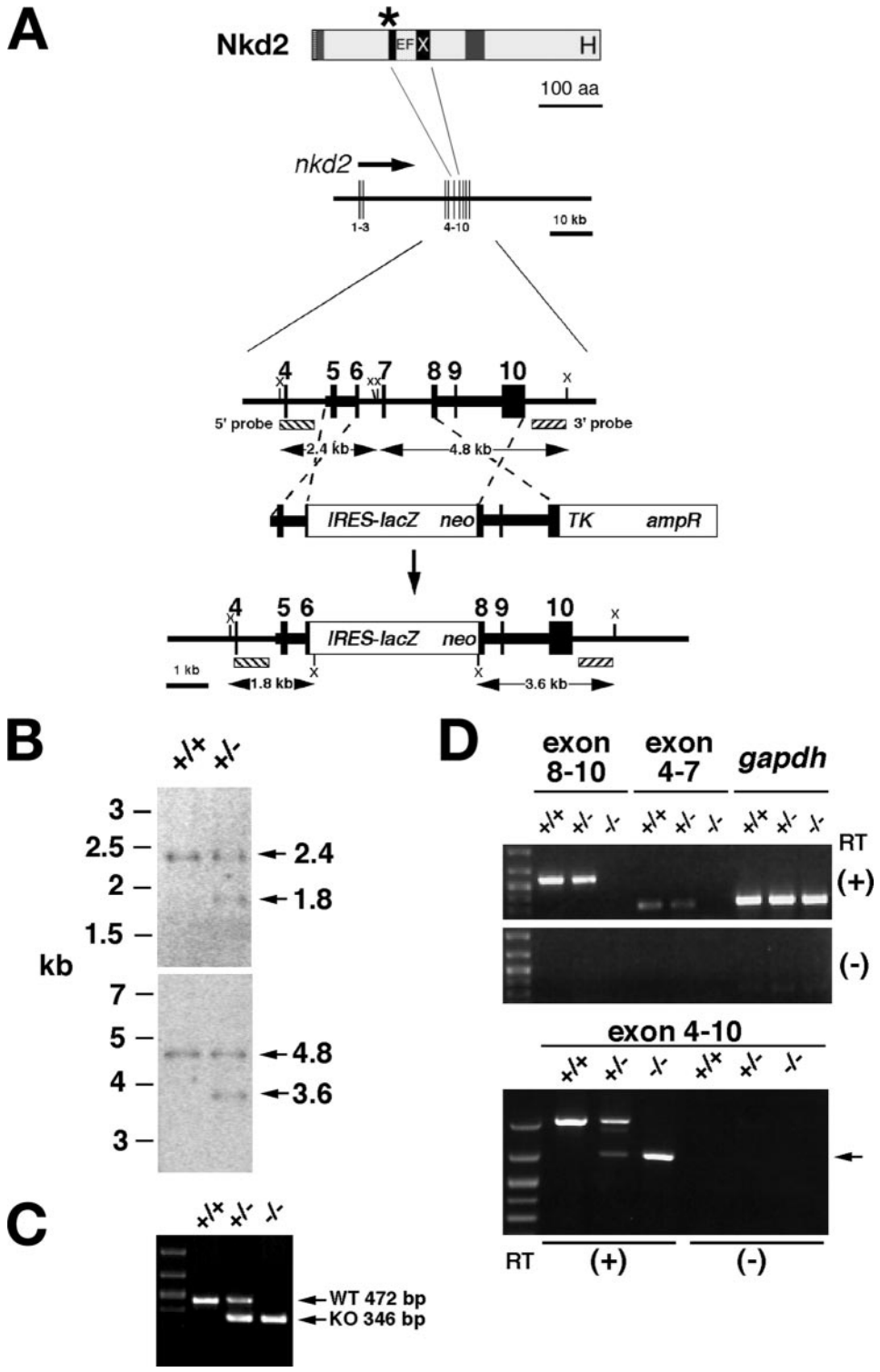

FIG. 2. Targeting of mouse *nkd2*. (A) Schematic of Nkd2 protein above the *nkd2* genomic region as described for Fig. 1. Homologous recombination replaced exons 6 to 8 with the *IRES-lacZ/neo* cassette. Enzyme site: X, XbaI. aa, amino acids. (B) Southern blotting of tail DNAs from mice of the indicated genotypes cut with XbaI (top and bottom) and probed with 5′ (top) or 3′ (bottom) external probes as designated in panel A. (C) PCR genotyping with tail DNA from mice of the indicated genotypes amplified by primers specific for the wild-type (WT) and *nkd2*^{lacZ} (KO) chromosomes. (D) RT-PCR analysis of brain RNA from adult mice of the indicated *nkd2* genotypes with primers spanning the designated *nkd2* exons or the control gene *gapdh*, with (+) or without (−) reverse transcriptase (RT). Markers are loaded in the leftmost lanes. (Top) −/− reactions lack specific bands spanning exons 8 to 10 (579 bp) or 4 to 7 (323 bp) that were deleted by the targeting event. *gapdh* (350 bp) is a positive control that is amplified from all three samples. (Bottom) +/+ mice have a 1,025-bp band corresponding to the full-length exon 4 to 10 product. +/− mice have 1,025- and 699-bp bands, while −/− mice only have the 699-bp band (arrow). Sequencing of the 699-bp band revealed exon 5-9-10 splicing, predicting the synthesis of an out-of-frame, truncated protein (data not shown).

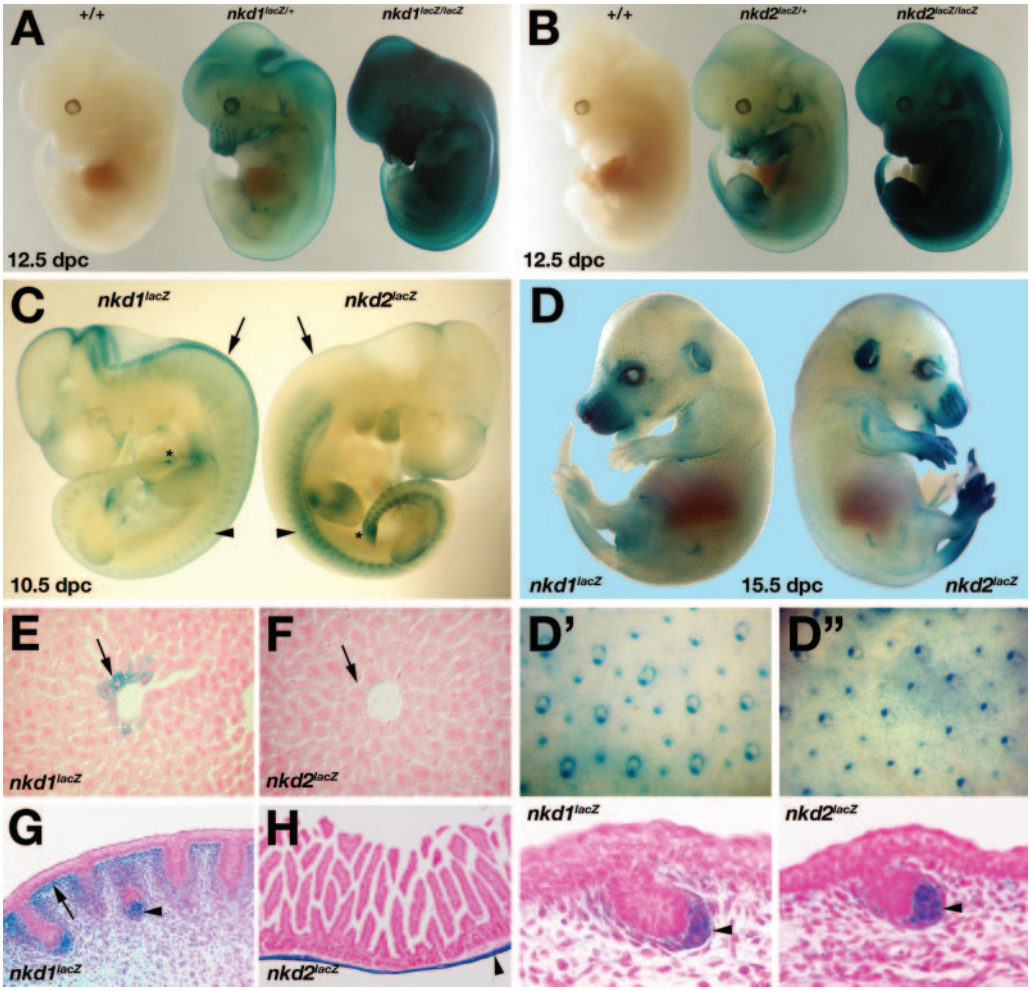

FIG. 3. Expression patterns of *nkd1*^{lacZ} and *nkd2*^{lacZ}. (A and B) X-Gal staining of 12.5-dpc embryos harvested from *nkd1*$^{lacZ/+}$ (A) or *nkd2*$^{lacZ/+}$ (B) heterozygous intercrosses reveals an intensity of blue staining that increases with the *nkd*^{lacZ} copy number. (C) Ten and one-half day postcoitus *nkd1*$^{lacZ/+}$ (left) or *nkd2*$^{lacZ/+}$ (right) embryo. Note dorsal CNS staining in *nkd1*^{lacZ} that is absent from *nkd2*^{lacZ} (arrows) but similar somite (arrowheads) and tail bud (asterisks) expression. (D) Fifteen and one-half day postcoitus *nkd1*$^{lacZ/+}$ (left) and *nkd2*$^{lacZ/+}$ (right) embryos. Note the similar expression of each gene in the snout, ear, and hair follicles (panels D′ to D″) but distinct staining patterns in the distal limb buds. (E and F) Liver tissue from adult *nkd1*$^{lacZ/+}$ (E) or *nkd2*$^{lacZ/+}$ (F) mice showing pericentral hepatocyte staining in the former but not the latter. (G) Snout tissue of a 15.5-dpc *nkd1*$^{lacZ/+}$ mouse showing expression in whisker mesenchyme (arrow) and dermal papillae (arrowhead). (H) *nkd2*$^{lacZ/+}$ mouse intestine tissue showing staining of the wall musculature (arrowhead).

Antibody Production Core and three made by Cell Signaling Technology; data not shown) at 4°C overnight, followed by incubation with horseradish peroxidase-conjugated goat anti-rabbit secondary antibodies (1:1,500; Pierce) at room temperature for 1 h. Signals were visualized with the SuperSignal West Chemiluminescent Substrate kit (Pierce).

X-Gal staining. Embryos and adult tissues were dissected in phosphate-buffered saline, fixed in 4% paraformaldehyde–phosphate-buffered saline for 1 h at 4°C, rinsed three times for 30 min each time in rinse buffer (100 mM sodium phosphate, 2 mM $MgCl_2$, 0.01% sodium deoxycholate, 0.02% NP-40), and then incubated in 5-bromo-4-chloro-3-indolyl-β-D-galactopyranoside (X-Gal) staining solution (100 mM sodium phosphate, 2 mM $MgCl_2$, 0.01% sodium deoxycholate, 0.02% NP-40, 5 mM potassium ferricyanide, 5 mM potassium ferrocyanide, 1 mg/ml X-Gal) overnight at 37°C to detect β-galactosidase activity. Sectioned X-Gal-stained tissues were counterstained in nuclear fast red.

Immunohistochemistry. β-Catenin immunostaining was performed in duplicate on testis tissue from three animals of each genotype at room temperature with the Animal Research Kit (Dako) and antigen retrieval reagent BORG (BioCare Medical). Anti-β-catenin monoclonal antibody E-5 (Santa Cruz Biotechnology) was used at 1:40, and slides were counterstained with hematoxylin.

Skeletal preparations. Adult mice of the ages indicated were euthanized by CO_2 inhalation, skinned, eviscerated, fixed in 95% ethanol overnight, and then rocked in acetone overnight to clear adipose tissues. The specimens were stained with alcian blue staining solution (4 volumes 95% ethanol, 1 volume acetic acid, and 0.15 mg alcian blue/ml) for 48 h, rinsed in 95% ethanol for >5 h, treated with 2% KOH overnight to remove soft tissues, and then stained with alizarin red staining solution (1% KOH plus 0.05 mg alizarin red/ml) for 30 to 90 min. The specimens were cleared in 1% KOH plus 20% glycerol for >2 days and then photographed in 50% ethanol–50% glycerol.

Dual-energy X-ray absorptiometry scans. Percent body fat and bone mineral density were determined with a GE-Lunar PIXImus equipped with software version 2.1.

Statistical analysis. The significance of mouse body and testis weights in Fig. 4 and 5B was calculated with a Student unpaired *t* test.

RESULTS

Targeting of the *nkd1* and *nkd2* genes. *nkd1* and *nkd2* are single-copy genes on mouse chromosomes 8C1 and 13C4, respectively; humans have single orthologs of each gene on chromosomes 16q12.1 and 5p15.3, with no additional closely re-

lated sequences or pseudogenes identified by genomic BLAST searches of the mouse and human genomes. In order to generate null mutations in *nkd1* and *nkd2*, we made mice harboring stop codons 5′ of each encoded EFX domain by replacing exons 5 to 10 (*nkd1*) or 6 to 8 (*nkd2*) with *IRES-lacZ* (Fig. 1A and 2A; see Materials and Methods). Southern blot assays, PCR, and genomic sequencing confirmed each targeting event, both in ES cells and following germ line transmission in mice (Fig. 1B and C and 2B and C and data not shown). Northern blotting and/or RT-PCR of tissues from homozygous mutant animals confirmed the predicted molecular nature of each targeting event (Fig. 1D and 2D and data not shown). Western analysis of 15.5-dpc embryo extracts of each *nkd1* genotype with affinity-purified anti-Nkd1 antisera confirmed the absence of Nkd1 protein in homozygous mutants (Fig. 1E). Unfortunately, four independent antisera against Nkd2 were unable to detect endogenous Nkd2 from either lysates or immunoprecipitates of 15.5-dpc embryos, despite the facts that *nkd2* mRNA and $nkd2^{lacZ}$ are abundant at that time and that each antiserum was able to detect overproduced Nkd2 by Western blotting of Nkd2-transfected cultured cells (70) (Fig. 3D and data not shown). We verified the homozygous viable nature of *nkd2* mutation by introducing a genetic lesion of comparable severity to $nkd2^{lacZ}$ by excising exon 5 via Cre-lox technology (T.C. and K.W., unpublished data).

$nkd1^{lacZ}$ and $nkd2^{lacZ}$ expression resembles endogenous *nkd* mRNA. As expected, the intensity of X-Gal staining in nkd^{lacZ} embryos or tissues strictly correlated with the gene dosage, with homozygous mutants consistently staining more intensely than heterozygotes (Fig. 3A and B). We observed patterns of X-Gal staining in each nkd^{lacZ} mouse that closely mimic the dynamic patterns of endogenous *nkd1* and *nkd2* mRNAs (e.g., cf. reference 70 and Fig. 3C), making each nkd^{lacZ} strain potentially useful as a reporter for Wnt-dependent transcriptional activity. For example, while $nkd1^{lacZ}$ and $nkd2^{lacZ}$ are each expressed in the somites and tail bud through mid-embryogenesis, $nkd1^{lacZ}$ but not $nkd2^{lacZ}$ is expressed in the dorsal embryonic CNS and in adult pericentral hepatocytes (Fig. 3C, E, and F), and both reporters are expressed in the intestinal musculature (Fig. 3H and data not shown). The expression of $nkd1^{lacZ}$ in some pericentral hepatocytes may reflect regulation by Wnt/β-catenin signals (6). By 15.5 dpc, $nkd1^{lacZ}$ and $nkd2^{lacZ}$ are expressed in similar patterns within the mesenchyme and dermal papillae of developing vibrissae and pelage hair follicles (Fig. 3D, D″, and G), where the roles for Wnt signaling in stem cell maintenance and follicle morphogenesis are well recognized (1).

***nkd1* or *nkd2* knockout mice are viable and fertile.** In a mixed 129-Bl6 genetic background, heterozygous intercrosses of each nkd^{lacZ} allele gave rise to viable progeny in roughly Mendelian ratios (Table 1) and animals homozygous mutant for each *nkd* allele were viable and fertile (Table 1). Growth curves for 4- to 12-week-old pups fed ad libitum showed a slight yet statistically significant retardation of growth (males, 15%; females, 4.6%) for $nkd1^{lacZ/lacZ}$ by 12 weeks, similar to a previously reported *nkd1* allele (45), but no growth abnormality in $nkd2^{lacZ/lacZ}$ (Fig. 4). Histology and weights of major organs from 3-month-old mice were comparable between the wild type and each mutant (n = 6 to 11 animals of each genotype; data not shown). We then crossed our original allele-transmitting chimeras into the 129SvEv background and found that heterozygous intercrosses of mice carrying each *nkd* allele also yielded roughly Mendelian progeny ratios but reduced mean litter sizes relative to the mixed background (Table 1).

TABLE 1. Breeding results from $nkd1^{lacZ}$ and $nkd2^{lacZ}$ crosses[a]

Background and cross	No. of pairs	No. of litters	No. of pups/litter	No. of mice of each genotype		
				+/+	+/−	−/−
Bl6–129 hybrid						
$nkd1^{lacZ/+} \times nkd1^{lacZ/+}$	9	15	7.3	32	55	23
$nkd2^{lacZ/+} \times nkd2^{lacZ/+}$	5	14	7.4	25	52	26
129						
$nkd1^{lacZ/+} \times nkd1^{lacZ/+}$	10	23	4.9	29	50	27
$nkd2^{lacZ/+} \times nkd2^{lacZ/+}$	3	4	5.8	9	7	7
Total (both)						
$nkd1^{lacZ/+} \times nkd1^{lacZ/+}$				61	105	50
$nkd2^{lacZ/+} \times nkd2^{lacZ/+}$				34	59	33
Bl6–129 hybrid						
$nkd1^{lacZ/lacZ} \times nkd1^{lacZ/lacZ}$	6	19	5.3			
$nkd2^{lacZ/lacZ} \times nkd2^{lacZ/lacZ}$	9	33	6.4			
129						
$nkd1^{lacZ/lacZ} \times nkd1^{lacZ/lacZ}$[b]	6	1	1			
$nkd2^{lacZ/lacZ} \times nkd2^{lacZ/lacZ}$	6	20	4.5			

[a] For each cross, the number of breeding pairs, the number of litters, and the mean number of pups per litter are indicated.

[b] Among six breeding pairs, a single litter consisting of a single pup was produced during a 3-month period. No histologic abnormalities were noted in the testes or ovaries of $nkd1^{lacZ/lacZ}$ animals in the 129 background, although one of the males had unilateral testicular agenesis.

$nkd1^{lacZ/lacZ}$ and $nkd2^{lacZ/lacZ}$ mice in a mixed background were fertile but with slightly reduced mean litter sizes compared to those of heterozygotes (Table 1). In view of the important role for Wnt/β-catenin signaling in the maintenance of bone mass (21, 38), examination of alizarin red- and alcian blue-stained 3-month-old female skeletons (two wild type, four $nkd1^{lacZ/lacZ}$, and two $nkd2^{lacZ/lacZ}$), as well as dual-energy X-ray absorptiometry scans and subsequent histologic sections of knee joints (four wild type, five $nkd1^{lacZ/lacZ}$, and five $nkd2^{lacZ/lacZ}$), did not yield any consistent differences between wild-type and *nkd1* or *nkd2* mutant animals (data not shown).

In the course of our studies, another group reported that homozygosity for a distinct targeted mutation in *nkd1* caused a slight reduction in testis size and reduced numbers of elongated sperm (45). In contrast to their report, our 3-month-old $nkd1^{lacZ/lacZ}$ (and $nkd2^{lacZ/lacZ}$) mice had testis-to-body weight ratios similar to those of the wild type (Fig. 5B). X-Gal staining of mutant testis tissue revealed β-galactosidase activity in elongating spermatids within testicular tubules (Fig. 5C to E), consistent with previous observations (45). However, in contrast to the previously reported *nkd1* mutant mice, we did not observe any obvious differences in β-catenin abundance or distribution by diaminobenzidine (DAB) immunohistochemistry between wild-type and *nkd1* or *nkd2* mutant testes (three testes per genotype) (Fig. 5F to H). Unlike our knockout alleles, which are each predicted to encode proteins truncated near their N termini, the previously reported *nkd1* allele encodes an internally deleted ~45-kDa Nkd1 protein that lacks the Dvl-binding EFX domain, and its persistence in the previously reported

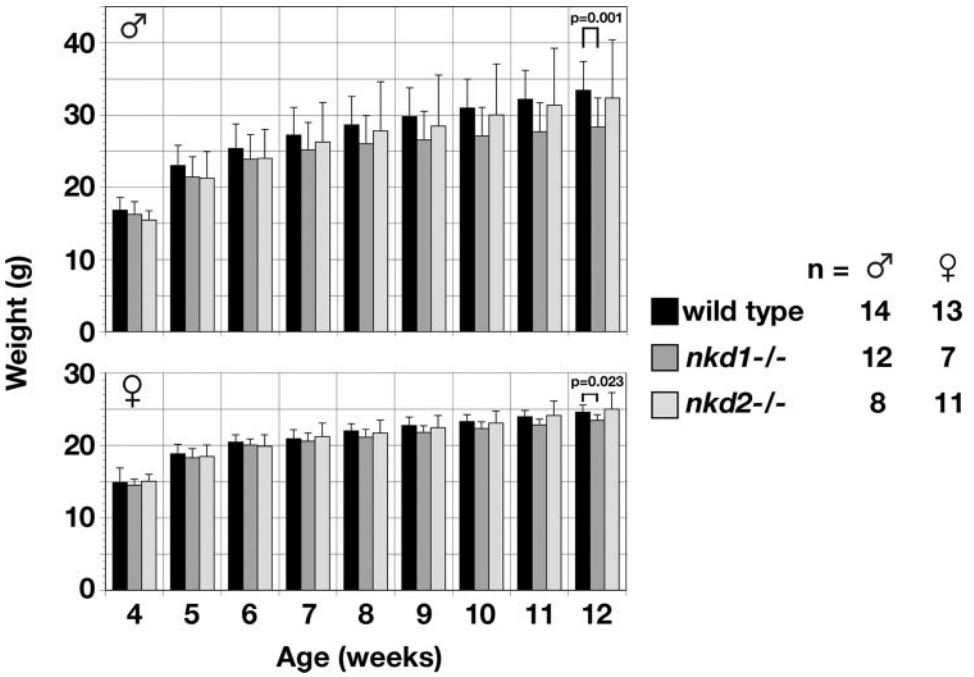

FIG. 4. Growth curves of wild-type and *nkd1* and *nkd2* mutant mice. Shown are mean weights ± standard deviations for the indicated numbers of male (top) and female (bottom) mice at the indicated postnatal weeks of age. At 12 weeks, $nkd1^{lacZ/lacZ}$ but not $nkd2^{lacZ/lacZ}$ mice are significantly smaller than wild-type mice, with *P* values indicated.

knockouts (45) may interfere with Wnt/β-catenin signaling and/or Dvl homeostasis in a manner distinct from that of our mutations.

***nkd1 nkd2* double-knockout mice are viable.** *nkd1* and *nkd2* are expressed in partially redundant patterns throughout gestation (e.g., Fig. 3D), so the absence of visible embryonic phenotypes could be due to genetic redundancy. To test this possibility, we mated $nkd1^{lacZ}$ and $nkd2^{lacZ}$ mice in the mixed genetic background. $nkd1^{lacZ/+}$ $nkd2^{lacZ/+}$ mice were viable and fertile, as were their progeny with the genotypes $nkd1^{lacZ/lacZ}$ $nkd2^{lacZ/+}$, $nkd1^{lacZ/+}$ $nkd2^{lacZ/lacZ}$, and $nkd1^{lacZ/lacZ}$ $nkd2^{lacZ/lacZ}$. However, females possessing no or one wild-type copy of *nkd1* or *nkd2* did not tend to their young as well as *nkd1* or *nkd2* homozygous mutants, as 35% of 46 litters from mothers with no or one wild-type copy of *nkd1* or *nkd2* were cannibalized by their mothers prior to weaning, compared to 14% of 51 litters from $nkd1^{lacZ/lacZ}$ or $nkd2^{lacZ/lacZ}$ single-mutant mothers. Nevertheless, by breeding male and female compound heterozygous mice, we raised two male and three female $nkd1^{lacZ/lacZ}$ $nkd2^{lacZ/lacZ}$ mice from 12 litters, confirming their genotype by PCR and Southern blotting (e.g., Fig. 6A to C). No histologic abnormalities were observed in major organs of the five double-knockout mice obtained (data not shown), and the abundance and distribution of β-catenin by DAB immunohistochemistry in double-knockout testes resembled the wild type and the single mutants (Fig. 5F to I). However, skeletal preparations of male and female 2-month-old double-knockout mice revealed a slightly shortened skull and nasal bones (Fig. 6D and data not shown) that are similar to but less severe than those of animals homozygous mutant for another antagonist of Wnt/β-catenin signaling, *axin2* (46, 73). While *axin2* mutant cranial bone sutures underwent premature fusion (73) in a manner that is perhaps similar to human craniosynostosis, such fusions were not evident in the two *nkd* double-knockout animals examined (Fig. 6D and data not shown), suggesting that the *nkd* mutant phenotype is not as severe as that of *axin2*.

DISCUSSION

The discovery of a discrete "toolkit" of conserved genes that govern the development of all animals was one of the great epiphanies of 20th century biology. Wnt proteins are among the most ancient of the toolkit proteins and remain a subject of intense biomedical interest not only for their roles in a diverse array of physiological processes but also due to frequent misregulation of Wnt signaling in human disease. The widespread activation of Wnt, Hedgehog, EGF, and Notch signaling in human cancer underscores each cell's critical task of controlling these signaling systems in their normal contexts, where they enforce stem cell and tissue homeostasis (9, 28, 64). Multiple control mechanisms have evolved to ensure that each of these influential signals is active only at the right place and for a limited time. In addition to restricting the synthesis of pathway-stimulating ligands, feedback regulation is a key mechanism that limits the action of these signals (17).

Our previous work showed that *nkd* is a negative feedback regulator for Wg signaling in *Drosophila* and that mice and humans have two *nkd*-related genes, *nkd1* and *nkd2* (70, 75). Guided by our studies of *Drosophila nkd* function, we generated early truncating lesions in each mouse *nkd* gene to investigate whether they are essential for development. To our surprise, *nkd* genes are dispensable for mouse development, as we only observed subtly reduced fertility, increased cannibal-

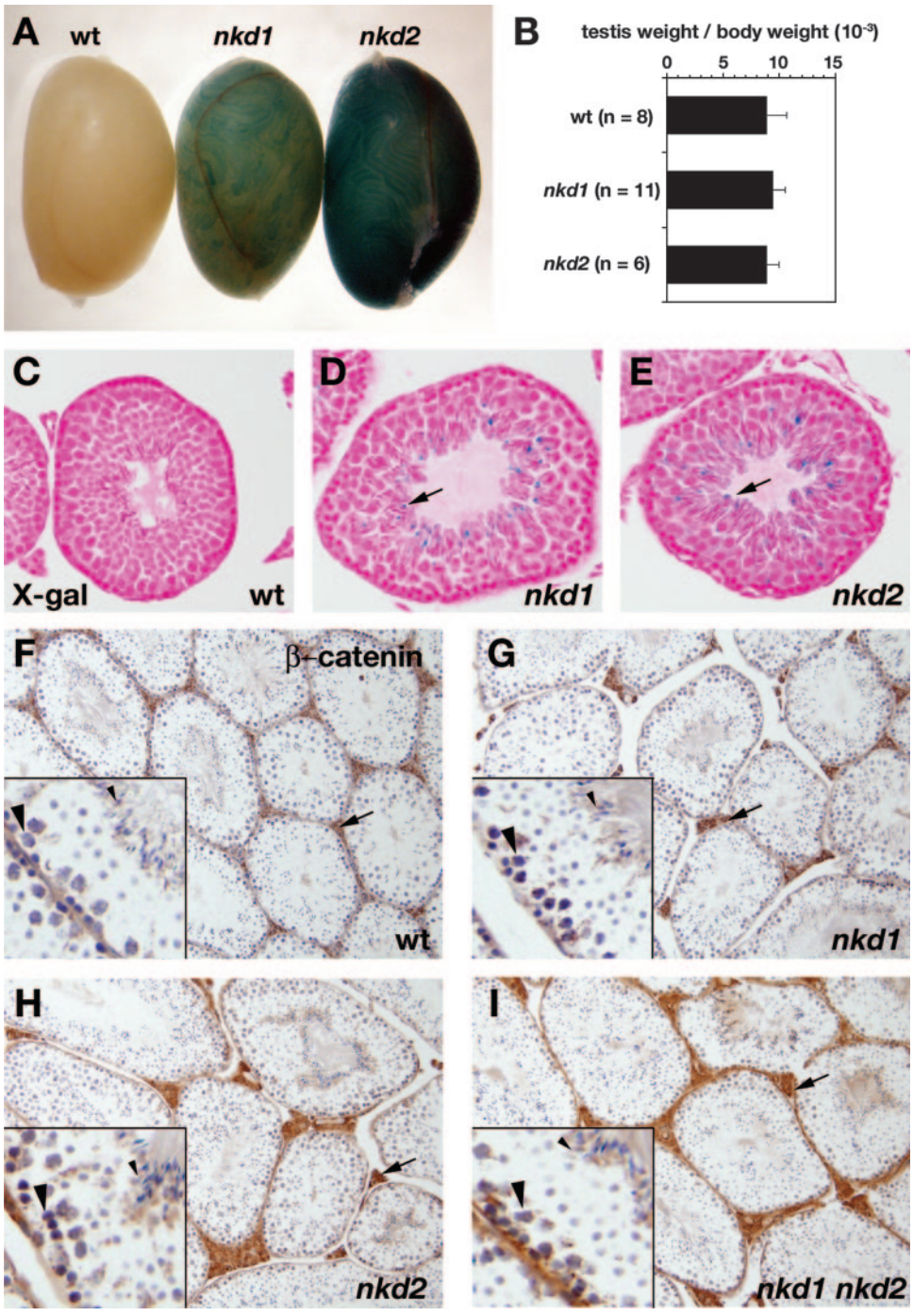

FIG. 5. *nkd* mutant testes resemble wild-type testes. (A) X-Gal-stained wild-type (wt, left), $nkd1^{lacZ/lacZ}$ (middle), and $nkd2^{lacZ/lacZ}$ (right) testis tissues from 3-month-old males. (B) Ratios of combined testis weight to body weight for the indicated numbers of 3-month-old wild-type (top bar) and homozygous *nkd1* (middle bar) or *nkd2* (bottom bar) mutant male mice. (C to E) High-power magnifications of X-Gal-stained testis tubules from wild-type (C), $nkd1^{lacZ/lacZ}$ (D), and $nkd2^{lacZ/lacZ}$ (E) mice. Note the X-Gal-positive elongating sperm near the tubular lumen (arrows) in panels D and E. (F to I) β-Catenin immunohistochemistry of wild-type (F), $nkd1^{lacZ/lacZ}$ (G), $nkd2^{lacZ/lacZ}$ (H), and $nkd1^{lacZ/lacZ}$ $nkd2^{lacZ/lacZ}$ (I) testes revealed by DAB staining (brown) shows similar distribution and intensity of intertubular (Leydig cell, arrow) staining, as well as basal spermatocyte nuclei (large arrowhead in lower left of each inset) and elongating spermatids (small arrowhead in upper right of each inset). Note the similar staining of all four genotypes.

ization of litters, and altered cranial bone morphology in mutant animals. We surmise that each of these phenotypes is modifiable by genetic background, as litter sizes were consistently reduced in the pure 129 background compared to the mixed Bl6-129 background. We also observed shortened nasal bones in $nkd1^{lacZ/lacZ}$ single-mutant animals in the 129 background—similar to those seen in the double-knockout animals in the mixed background—which was not evident for $nkd1^{lacZ/lacZ}$ in

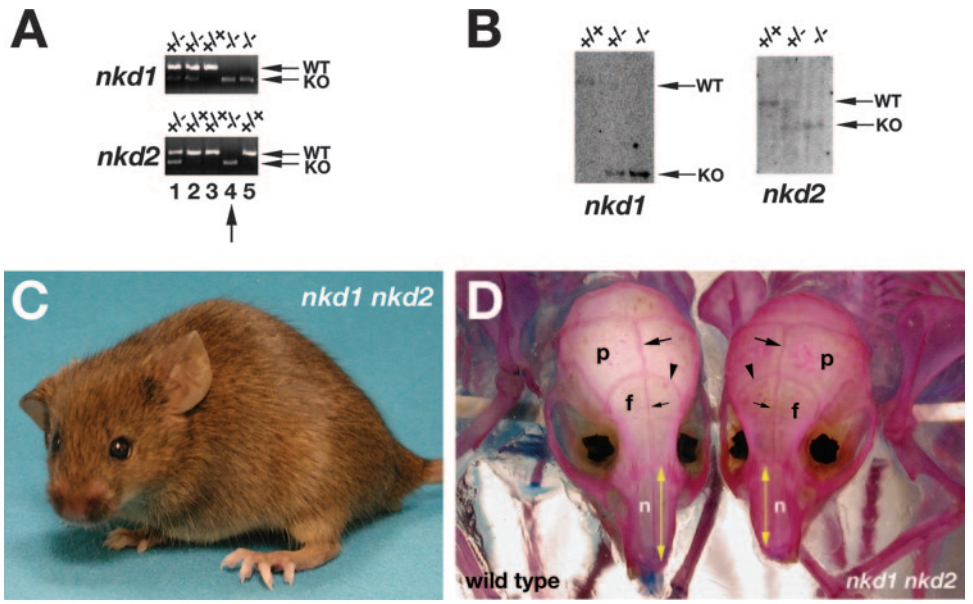

FIG. 6. *nkd1 nkd2* double-mutant mice are viable. (A) PCR genotyping of a subset of progeny of an $nkd1^{lacZ/+}$ $nkd2^{lacZ/+}$ intercross for *nkd1* and *nkd2* gene status. Note that lane 4 DNA is from a double knockout. WT, wild type; KO, knockout. (B) Southern blotting of wild-type (left lanes), $nkd1^{lacZ/+}$ $nkd2^{lacZ/+}$ (middle lanes), and $nkd1^{lacZ/lacZ}$ $nkd2^{lacZ/lacZ}$ (right lanes) DNAs probed for *nkd1* (left blot) and *nkd2* (right blot) status. (C) Three-month-old $nkd1^{lacZ/lacZ}$ $nkd2^{lacZ/lacZ}$ adult female with a slightly short nose. (D) Rostral view of wild-type (left) and $nkd1^{lacZ/lacZ}$ $nkd2^{lacZ/lacZ}$ (right) 2-month-old female skeleton preparations. Cranial bones: parietal (p), frontal (f), and nasal (n). Sutures: sagittal (large arrows), coronal (arrowheads), and posterior frontal (small arrows). The double line of alizarin red stain at sutures suggests an absence of craniosynostosis. Note that the length of the nasal bone, from the frontonasal suture to its anterior tip, is decreased in an $nkd1^{lacZ/lacZ}$ $nkd2^{lacZ/lacZ}$ mouse (double yellow arrows).

the mixed background (data not shown), indicating that the cranial abnormalities in our *nkd* mutants are also strain dependent.

The similarity between *nkd*- and *axin2*-encoded mutant cranial phenotypes is likely not a coincidence because both genes are inducible inhibitors of Wnt/β-catenin signaling (50). Mice express another *axin* gene, *axin1*, that is not regulated by Wnt signaling but which is essential for early development (74). Any differences in *axin1* and *axin2* function are the result of distinct expression patterns, because the endogenous mouse *axin1* coding region can be replaced with the *axin2* cDNA without phenotypic consequence (10). It is intriguing that just as our *nkd* mutant mouse phenotype is less severe than the *axin2* phenotype, the cuticle phenotype of *Drosophila nkd* mutants is typically not as severe as that of *axin* mutants (23, 34, 67). Genetic epistasis has also revealed an important difference between the *nkd* and *axin* genes in *Drosophila*, with the *nkd* phenotype being signal dependent and *axin* signal independent (5, 23, 57). If this relationship is also true in mammals, then one may predict that the *nkd* mutant but not the *axin2* mutant phenotype should be suppressed by reducing the *wnt* or *dvl* gene dosage. In spite of this conjecture, the *axin2* mutant cranial phenotype is partially suppressed by heterozygosity for β-*catenin* (46), consistent with *axin1*-dependent regulation of β-catenin levels in *axin2* mutant adults.

If the mouse *nkd* genes are dispensable for development, then why are they conserved in evolution? Let us first reconsider the function of *nkd* in *Drosophila*. Early in fly development, just prior to the time when Wg is active, *nkd* is broadly transcribed in the embryo (75). *nkd* accumulation in proportion to the Wg signal then limits β-catenin accumulation and Wg target gene expression (14, 42, 43, 52, 62, 75). Despite the complex, Wg-dependent striped pattern of *nkd* expression evident during segmentation, ubiquitous Nkd can rescue an *nkd* mutant to adulthood, indicating that *nkd* regulation by Wg signaling is not strictly necessary for Nkd activity (67). In an otherwise wild-type background, Nkd overproduction had little effect on the fly embryo pattern (33, 75). Similarly, we were unable to observe any obvious consequences for development or physiology when mouse Nkd1 was expressed in transgenic mice under the control of the ubiquitous elongation factor 1-α promoter or the inducible metallothionein promoter (M. Zhang, M. Amanai, and K. A. Wharton, Jr., unpublished observations). However, in *Drosophila*, severe loss-of-Wg signaling phenotypes can be induced in the embryo when Nkd is overproduced in a genetic background compromised for Wg pathway activity (33, 75) or when Nkd is overproduced through several days of larval and pupal development, resulting in a spectrum of adult phenotypes indicative of reduced Wg signaling or *dsh* activity (57, 75). Thus, it is possible that our *nkd1* transgenes were unable to drive expression to levels high enough to produce visible phenotypes and/or that mammalian Nkd1 is an intrinsically weaker antagonist of Wnt signaling than *Drosophila* Nkd, as we have observed when either is misexpressed in *Drosophila* or *Xenopus* (70, 75; P. S. Klein, unpublished observation).

In a fashion reminiscent of the Wg-dependent expression of *nkd* in the fly, each mouse *nkd* gene is expressed in dynamic, gradient-like patterns throughout embryonic development, presumably as a consequence of regulation by Wnt and other signaling pathways (13, 31, 59, 70). In addition to a common

organization of sequence motifs in all known Nkd proteins (67), the exquisite conservation of several putative ion chelation residues in the "loop" of the EFX domain in all of the Nkd proteins sequenced to date (70, 75; K.W., unpublished data) strongly suggests conserved functions involving Dsh/Dvl and possibly other proteins that associate with this domain. However, a mutant Nkd protein—albeit overproduced—that lacks the EFX domain can rescue a fly *nkd* mutant (67), indicating that the EFX domain, at least in *Drosophila*, is not strictly required for Nkd activity. The present study also shows that Nkd EFX domains are not required for mouse development; however, in contrast to the situation in the fly (67), we show that the mouse *nkd* genes are themselves dispensable for embryonic development.

At least three hypotheses to account for the present results can be entertained. First, an absolute requirement for the *nkd* genes may not be revealed when breeding mice in a controlled environment under artificial selection. Consistent with this idea is our observation that mothers with no or one residual copy of wild-type *nkd* had an increased propensity to cannibalize their young after birth, suggesting behavioral or stress-related reproductive phenotypes that will be the subject of future investigation.

A second possibility is that any alterations in Wnt/β-catenin signaling that arise in animals lacking *nkd* activity during embryonic development may be compensated for by altered expression of other Wnt pathway antagonists, such as those of the secreted Frizzled-related protein (sFRP), Cerberus, WIF, and Dickkopf (Dkk) families, which act extracellularly (36), or Axin2 and Lef1, which act intracellularly (26, 44, 50, 72). Indeed, the requirement for *nkd* in *Drosophila* may be absolute because flies do not possess homologs of the extracellular antagonist sFRP, Cerberus, or Dkk families, and the lone *Drosophila* WIF protein is dedicated to regulating Hh and not Wnt signaling (20, 22). In contrast to the mammalian genes, there have been no reports of transcriptional regulation of the *Drosophila axin* or *tcf* gene, and other genes such as *wingful* and *notum* appear to play more important roles in regulating postembryonic Wg signaling than *nkd* (18, 19, 75).

Finally, the function of *nkd* genes and their likely retention throughout much of the animal kingdom may be rooted in the phenomenon of canalization, a term that describes the capacity of evolved life to minimize phenotypic variation in the face of perturbations in the environment or genetic background (66; reviewed in reference 15). The mammalian *nkd* genes may fine-tune the levels and/or activities of the Dvl proteins so that downstream signaling events occur with high fidelity. Thus, a strict requirement for *nkd* genes may be revealed by experiments that measure the extent to which *nkd* mutant animals are susceptible to genetic or pharmacologic perturbation in Wnt or Dvl signaling. Future behavioral experiments, or experiments in which mutations in the murine *nkd* genes are combined with mutations in other Wnt signaling regulators, may reveal additional roles for these evolutionarily well-conserved genes.

ACKNOWLEDGMENTS

Special thanks go to Matthew Scott, in whose laboratory the genomic characterization of murine *nkd* genes was initiated. Thanks go to Jon Graff for the targeting vector; Robert Hammer, Robin Nguyen, and John Ritter for expert ES cell culture and chimeric-mouse production; Makoto Kuro-O and Ljiljana Milenkovic for transgenic mouse vectors; Jim Richardson and John Shelton for histology; Wayne Lai and the UT Southwestern Antibody Core for antibodies; Xiaowu Zhang and Cell Signaling Technology for generously providing anti-Nkd1 and anti-Nkd2 antibodies; Mike Arnold, Yuri Kim, and Eric Olson for advice regarding skeletal preparations; Kevin White for introducing K.A.W. to the concept of canalization; and Chih-Chiang Chan, Jin Jiang, and Robert Hammer for comments on the manuscript.

K.A.W. acknowledges Matthew Scott for support of J.K. by the Howard Hughes Medical Institute. K.A.W. is a W. W. Caruth, Jr., Scholar in Biomedical Research at UT Southwestern and has received support from the Texas affiliate of the American Heart Association, an Institutional Junior Faculty Research Grant from the American Cancer Society, UT Southwestern Dean's funds, the Department of Pathology, NIH K08-HD01164, and R01-GM65404.

REFERENCES

1. **Alonso, L., and E. Fuchs.** 2003. Stem cells in the skin: waste not, Wnt not. Genes Dev. **17:**1189–1200.
2. **Artavanis-Tsakonas, S., K. Matsuno, and M. E. Fortini.** 1995. Notch signaling. Science **268:**225–232.
3. **Baker, N. E.** 1988. Localization of transcripts from the *wingless* gene in whole *Drosophila* embryos. Development **103:**289–298.
4. **Bejsovec, A., and A. Martinez Arias.** 1991. Roles of *wingless* in patterning the larval epidermis of *Drosophila*. Development **113:**471–485.
5. **Bejsovec, A., and E. Wieschaus.** 1993. Segment polarity gene interactions modulate epidermal patterning in *Drosophila* embryos. Development **119:** 501–517.
6. **Benhamouche, S., T. Decaens, C. Godard, R. Chambrey, D. S. Rickman, C. Moinard, M. Vasseur-Cognet, C. J. Kuo, A. Kahn, C. Perret, and S. Colnot.** 2006. *Apc* tumor suppressor gene is the "zonation-keeper" of mouse liver. Dev. Cell **10:**759–770.
7. **Boutros, M., and M. Mlodzik.** 1999. Dishevelled: at the crossroads of divergent intracellular signaling pathways. Mech. Dev. **83:**27–37.
8. **Carroll, S. B., J. K. Grenier, and S. D. Weatherbee.** 2001. From DNA to diversity: molecular genetics and the evolution of animal design. Blackwell Science, Inc., Malden, MA.
9. **Casci, T., and M. Freeman.** 1999. Control of EGF receptor signalling: lessons from fruitflies. Cancer Metastasis Rev. **18:**181–201.
10. **Chia, I. V., and F. Costantini.** 2005. Mouse axin and axin2/conductin proteins are functionally equivalent in vivo. Mol. Cell. Biol. **25:**4371–4376.
11. **Clevers, H.** 2006. Wnt/β-catenin signaling in development and disease. Cell **127:**469–480.
12. **Couso, J. P., and A. Martinez Arias.** 1994. *Notch* is required for *wingless* signaling in the epidermis of Drosophila. Cell **79:**259–272.
13. **Dequeant, M. L., E. Glynn, K. Gaudenz, M. Wahl, J. Chen, A. Mushegian, and O. Pourquie.** 2006. A complex oscillating network of signaling genes underlies the mouse segmentation clock. Science **314:**1595–1598.
14. **DiNardo, S., J. M. Kuner, J. Theis, and P. H. O'Farrell.** 1985. Development of embryonic pattern in *D. melanogaster* as revealed by accumulation of the nuclear engrailed protein. Cell **43:**59–69.
15. **Flatt, T.** 2005. The evolutionary genetics of canalization. Q. Rev. Biol. **80:**287–316.
16. **Fradkin, L. G., M. van Schie, R. R. Wouda, A. de Jong, J. T. Kamphorst, M. Radjkoemar-Bansraj, and J. N. Noordermeer.** 2004. The *Drosophila* Wnt5 protein mediates selective axon fasciculation in the embryonic central nervous system. Dev. Biol. **272:**362–375.
17. **Freeman, M.** 2000. Feedback control of intercellular signalling in development. Nature **408:**313–319.
18. **Gerlitz, O., and K. Basler.** 2002. Wingful, an extracellular feedback inhibitor of Wingless. Genes Dev. **16:**1055–1059.
19. **Giraldez, A. J., R. R. Copley, and S. M. Cohen.** 2002. HSPG modification by the secreted enzyme Notum shapes the Wingless morphogen gradient. Dev. Cell **2:**667–676.
20. **Glise, B., C. A. Miller, M. Crozatier, M. A. Halbisen, S. Wise, D. J. Olson, A. Vincent, and S. S. Blair.** 2005. Shifted, the *Drosophila* ortholog of Wnt inhibitory factor-1, controls the distribution and movement of Hedgehog. Dev. Cell **8:**255–266.
21. **Gong, Y., R. B. Slee, N. Fukai, G. Rawadi, S. Roman-Roman, A. M. Reginato, H. Wang, T. Cundy, F. H. Glorieux, D. Lev, M. Zacharin, K. Oexle, J. Marcelino, W. Suwairi, S. Heeger, G. Sabatakos, S. Apte, W. N. Adkins, J. Allgrove, M. Arslan-Kirchner, J. A. Batch, P. Beighton, G. C. Black, R. G. Boles, L. M. Boon, C. Borrone, H. G. Brunner, G. F. Carle, B. Dallapiccola, A. De Paepe, B. Floege, M. L. Halfhide, B. Hall, R. C. Hennekam, T. Hirose, A. Jans, H. Juppner, C. A. Kim, K. Keppler-Noreuil, A. Kohlschuetter, D. LaCombe, M. Lambert, E. Lemyre, T. Letteboer, L. Peltonen, R. S. Ramesar, M. Romanengo, H. Somer, E. Steichen-Gersdorf, B. Steinmann, B. Sullivan, A. Superti-Furga, W. Swoboda, M. J. van den Boogaard, W. Van Hul, M.**

Vikkula, M. Votruba, B. Zabel, T. Garcia, R. Baron, B. R. Olsen, and M. L. Warman. 2001. LDL receptor-related protein 5 (LRP5) affects bone accrual and eye development. Cell **107:**513–523.
22. **Gorfinkiel, N., J. Sierra, A. Callejo, C. Ibanez, and I. Guerrero.** 2005. The *Drosophila* ortholog of the human Wnt inhibitor factor Shifted controls the diffusion of lipid-modified Hedgehog. Dev. Cell **8:**241–253.
23. **Hamada, F., Y. Tomoyasu, Y. Takatsu, M. Nakamura, S. Nagai, A. Suzuki, F. Fujita, H. Shibuya, K. Toyoshima, N. Ueno, and T. Akiyama.** 1999. Negative regulation of Wingless signaling by *D-axin*, a *Drosophila* homolog of *axin*. Science **283:**1739–1742.
24. **Hatini, V., and S. DiNardo.** 2001. Divide and conquer: pattern formation in *Drosophila* embryonic epidermis. Trends Genet. **17:**574–579.
25. **Hing, H. K., X. Sun, and S. Artavanis-Tsakonas.** 1994. Modulation of *wingless* signaling by *Notch* in *Drosophila*. Mech. Dev. **47:**261–268.
26. **Hovanes, K., T. W. Li, J. E. Munguia, T. Truong, T. Milovanovic, J. Lawrence Marsh, R. F. Holcombe, and M. L. Waterman.** 2001. β-Catenin-sensitive isoforms of lymphoid enhancer factor-1 are selectively expressed in colon cancer. Nat. Genet. **28:**53–57.
27. **Hurley, I., M. E. Hale, and V. E. Prince.** 2005. Duplication events and the evolution of segmental identity. Evol. Dev. **7:**556–567.
28. **Hynes, N. E., and H. A. Lane.** 2005. ERBB receptors and cancer: the complexity of targeted inhibitors. Nat. Rev. Cancer **5:**341–354.
29. **Ingham, P. W., and A. P. McMahon.** 2001. Hedgehog signaling in animal development: paradigms and principles. Genes Dev. **15:**3059–3087.
30. **Inoue, T., H. S. Oz, D. Wiland, S. Gharib, R. Deshpande, R. J. Hill, W. S. Katz, and P. W. Sternberg.** 2004. C. elegans *LIN-18* is a *Ryk* ortholog and functions in parallel to *LIN-17*/*Frizzled* in Wnt signaling. Cell **118:**795–806.
31. **Ishikawa, A., S. Kitajima, Y. Takahashi, H. Kokubo, J. Kanno, T. Inoue, and Y. Saga.** 2004. Mouse *Nkd1*, a Wnt antagonist, exhibits oscillatory gene expression in the PSM under the control of Notch signaling. Mech. Dev. **121:**1443–1453.
32. **Itoh, K., B. K. Brott, G. U. Bae, M. J. Ratcliffe, and S. Y. Sokol.** 2005. Nuclear localization is required for Dishevelled function in Wnt/β-catenin signaling. J. Biol. **4:**3.
33. **Jones, W. M., and A. Bejsovec.** 2005. *RacGap50C* negatively regulates *wingless* pathway activity during *Drosophila* embryonic development. Genetics **169:**2075–2086.
34. **Jürgens, G., E. Wieschaus, C. Nüsslein-Volhard, and H. Kluding.** 1984. Mutations affecting the pattern of the larval cuticle in *Drosophila melanogaster*. II. Zygotic loci on the third chromosome. Wilhelm Roux Arch. Dev. Biol. **193:**283–295.
35. **Katoh, M.** 2001. Molecular cloning, gene structure, and expression analyses of *NKD1* and *NKD2*. Int. J. Oncol. **19:**963–969.
36. **Kawano, Y., and R. Kypta.** 2003. Secreted antagonists of the Wnt signalling pathway. J. Cell Sci. **116:**2627–2634.
37. **Klingensmith, J., and R. Nusse.** 1994. Signaling by *wingless* in *Drosophila*. Dev. Biol. **166:**396–414.
38. **Koay, M. A., and M. A. Brown.** 2005. Genetic disorders of the LRP5-Wnt signalling pathway affecting the skeleton. Trends Mol. Med. **11:**129–137.
39. **Korswagen, H. C.** 2002. Canonical and non-canonical Wnt signaling pathways in *Caenorhabditis elegans*: variations on a common signaling theme. Bioessays **24:**801–810.
40. **Kühl, M.** 2004. The WNT/calcium pathway: biochemical mediators, tools and future requirements. Front. Biosci. **9:**967–974.
41. **Kusserow, A., K. Pang, C. Sturm, M. Hrouda, J. Lentfer, H. A. Schmidt, U. Technau, A. von Haeseler, B. Hobmayer, M. Q. Martindale, and T. W. Holstein.** 2005. Unexpected complexity of the *Wnt* gene family in a sea anemone. Nature **433:**156–160.
42. **Larsen, C. W., E. Hirst, C. Alexandre, and J. P. Vincent.** 2003. Segment boundary formation in *Drosophila* embryos. Development **130:**5625–5635.
43. **Lee, J. J., D. P. von Kessler, S. Parks, and P. A. Beachy.** 1992. Secretion and localized transcription suggest a role in positional signaling for products of the segmentation gene *hedgehog*. Cell **71:**33–50.
44. **Leung, J. Y., F. T. Kolligs, R. Wu, Y. Zhai, R. Kuick, S. Hanash, K. R. Cho, and E. R. Fearon.** 2002. Activation of *AXIN2* expression by β-catenin/TCF: a feedback repressor pathway regulating Wnt signaling. J. Biol. Chem. **277:**21657–21665.
45. **Li, Q., T. O. Ishikawa, H. Miyoshi, M. Oshima, and M. M. Taketo.** 2005. A targeted mutation of *Nkd1* impairs mouse spermatogenesis. J. Biol. Chem. **280:**2831–2839.
46. **Liu, B., H. M. Yu, and W. Hsu.** 2007. Craniosynostosis caused by *Axin2* deficiency is mediated through distinct functions of β-catenin in proliferation and differentiation. Dev. Biol. **301:**298–308.
47. **Logan, C. Y., and R. Nusse.** 2004. The Wnt signaling pathway in development and disease. Annu. Rev. Cell Dev. Biol. **20:**781–810.
48. **Louvi, A., and S. Artavanis-Tsakonas.** 2006. Notch signalling in vertebrate neural development. Nat. Rev. Neurosci. **7:**93–102.
49. **Lu, W., V. Yamamoto, B. Ortega, and D. Baltimore.** 2004. Mammalian Ryk is a Wnt coreceptor required for stimulation of neurite outgrowth. Cell **119:**97–108.
50. **Lustig, B., B. Jerchow, M. Sachs, S. Weiler, T. Pietsch, U. Karsten, M. van de Wetering, H. Clevers, P. M. Schlag, W. Birchmeier, and J. Behrens.** 2002. Negative feedback loop of Wnt signaling through upregulation of *conductin*/*axin2* in colorectal and liver tumors. Mol. Cell. Biol. **22:**1184–1193.
51. **Malbon, C. C., and H. Y. Wang.** 2006. Dishevelled: a mobile scaffold catalyzing development. Curr. Top. Dev. Biol. **72:**153–166.
52. **Martinez Arias, A., N. E. Baker, and P. W. Ingham.** 1988. Role of segment polarity genes in the definition and maintenance of cell states in the *Drosophila* embryo. Development **103:**157–170.
53. **Noordermeer, J., P. Johnston, F. Rijsewijk, R. Nusse, and P. A. Lawrence.** 1992. The consequences of ubiquitous expression of the *wingless* gene in the *Drosophila* embryo. Development **116:**711–719.
54. **Noordermeer, J., J. Klingensmith, N. Perrimon, and R. Nusse.** 1994. *dishevelled* and *armadillo* act in the *wingless* signalling pathway in *Drosophila*. Nature **367:**80–83.
55. **Nüsslein-Volhard, C., and E. Wieschaus.** 1980. Mutations affecting segment number and polarity in *Drosophila*. Nature **287:**795–801.
56. **Peifer, M., D. Sweeton, M. Casey, and E. Wieschaus.** 1994. Wingless signal and Zeste-white 3 kinase trigger opposing changes in the intracellular distribution of Armadillo. Development **120:**369–380.
57. **Rousset, R., J. A. Mack, K. A. Wharton, Jr., J. D. Axelrod, K. M. Cadigan, M. P. Fish, R. Nusse, and M. P. Scott.** 2001. *naked cuticle* targets *dishevelled* to antagonize Wnt signal transduction. Genes Dev. **15:**658–671.
58. **Sanson, B.** 2001. Generating patterns from fields of cells. Examples from *Drosophila* segmentation. EMBO Rep. **2:**1083–1088.
59. **Schmidt, C., A. Otto, G. Luke, P. Valasek, W. R. Otto, and K. Patel.** 2006. Expression and regulation of *Nkd-1*, an intracellular component of Wnt signalling pathway in the chick embryo. Anat. Embryol. **211:**525–534.
60. **Siegfried, E., T. B. Chou, and N. Perrimon.** 1992. *wingless* signaling acts through *zeste-white* 3, the *Drosophila* homolog of *glycogen synthase kinase-3*, to regulate *engrailed* and establish cell fate. Cell **71:**1167–1179.
61. **Siegfried, E., E. L. Wilder, and N. Perrimon.** 1994. Components of *wingless* signalling in *Drosophila*. Nature **367:**76–80.
62. **Tabata, T., S. Eaton, and T. B. Kornberg.** 1992. The *Drosophila hedgehog* gene is expressed specifically in posterior compartment cells and is a target of *engrailed* regulation. Genes Dev. **6:**2635–2645.
63. **Tada, M., M. L. Concha, and C. P. Heisenberg.** 2002. Non-canonical Wnt signalling and regulation of gastrulation movements. Semin. Cell Dev. Biol. **13:**251–260.
64. **Taipale, J., and P. A. Beachy.** 2001. The Hedgehog and Wnt signalling pathways in cancer. Nature **411:**349–354.
65. **Veeman, M. T., J. D. Axelrod, and R. T. Moon.** 2003. A second canon. Functions and mechanisms of β-catenin-independent Wnt signaling. Dev. Cell **5:**367–377.
66. **Waddington, C. H.** 1942. Canalization of development and the inheritance of acquired characters. Nature **150:**563–565.
67. **Waldrop, S., C. C. Chan, T. Cagatay, S. Zhang, R. Rousset, J. Mack, W. Zeng, M. Fish, M. Zhang, M. Amanai, and K. A. Wharton, Jr.** 2006. An unconventional nuclear localization motif is crucial for function of the *Drosophila* Wnt/wingless antagonist naked cuticle. Genetics **174:**331–348.
68. **Wallingford, J. B., and R. Habas.** 2005. The developmental biology of Dishevelled: an enigmatic protein governing cell fate and cell polarity. Development **132:**4421–4436.
69. **Wharton, K. A., Jr.** 2003. Runnin' with the Dvl: proteins that associate with Dsh/Dvl and their significance to Wnt signal transduction. Dev. Biol. **253:**1–17.
70. **Wharton, K. A., Jr., G. Zimmermann, R. Rousset, and M. P. Scott.** 2001. Vertebrate proteins related to Drosophila Naked Cuticle bind Dishevelled and antagonize Wnt signaling. Dev. Biol. **234:**93–106.
71. **Yan, D., J. B. Wallingford, T. Q. Sun, A. M. Nelson, C. Sakanaka, C. Reinhard, R. M. Harland, W. J. Fantl, and L. T. Williams.** 2001. Cell autonomous regulation of multiple Dishevelled-dependent pathways by mammalian Nkd. Proc. Natl. Acad. Sci. USA **98:**3802–3807.
72. **Yan, D., M. Wiesmann, M. Rohan, V. Chan, A. B. Jefferson, L. Guo, D. Sakamoto, R. H. Caothien, J. H. Fuller, C. Reinhard, P. D. Garcia, F. M. Randazzo, J. Escobedo, W. J. Fantl, and L. T. Williams.** 2001. Elevated expression of *axin2* and *hnkd* mRNA provides evidence that Wnt/β-catenin signaling is activated in human colon tumors. Proc. Natl. Acad. Sci. USA **98:**14973–14978.
73. **Yu, H. M., B. Jerchow, T. J. Sheu, B. Liu, F. Costantini, J. E. Puzas, W. Birchmeier, and W. Hsu.** 2005. The role of *Axin2* in calvarial morphogenesis and craniosynostosis. Development **132:**1995–2005.
74. **Zeng, L., F. Fagotto, T. Zhang, W. Hsu, T. J. Vasicek, W. L. Perry III, J. J. Lee, S. M. Tilghman, B. M. Gumbiner, and F. Costantini.** 1997. The mouse *Fused* locus encodes *Axin*, an inhibitor of the Wnt signaling pathway that regulates embryonic axis formation. Cell **90:**181–192.
75. **Zeng, W., K. A. Wharton, Jr., J. A. Mack, K. Wang, M. Gadbaw, K. Suyama, P. S. Klein, and M. P. Scott.** 2000. *naked cuticle* encodes an inducible antagonist of Wnt signalling. Nature **403:**789–795.
76. **Zhu, Y., J. A. Richardson, L. F. Parada, and J. M. Graff.** 1998. *Smad3* mutant mice develop metastatic colorectal cancer. Cell **94:**703–714.